As originally published in the IPC proceedings.

Pad Cratering Susceptibility Testing with Acoustic Emission

Wong Boon San
Agilent Technologies, Bayan Lepas, Malaysia
Richard Nordstrom, Ph.D.
Acoustic Technology Group, Grandville, Michigan
Julie Silk
Agilent Technologies, Santa Rosa, California

Abstract
Pad cratering test methods have been under development with the emergence of this laminate fracture defect mechanism. In additional to ball shear, ball pull, and pin pull testing methods, the acoustic emission method is being developed to evaluate laminate materials' resistance to pad cratering. Though the acoustic emission (AE) method has been proven to be able to detect pad cratering, no study has reported which AE parameters are good indicators for the susceptibility of PCB laminates to pad cratering. In this study, six different laminates subjected to three different pre-conditioning (multiple reflow) cycles have undergone the four-point bend testing. Four AE sensors were used to monitor pad cratering during the bend test. Several AE parameters including amplitude in dB level, the energy, and the location of each AE event under different load levels are recorded. Location analysis shows the majority of AE events are concentrated in the largest BGA package in the test vehicle, which indicates that pad cratering is elevated with the larger size of BGA package due to high stress concentration. Both the number of AE events and the cumulative energy of AE events at a given applied load show that Laminate F is prone to pad cratering. However, there is no statistically significant difference in the lowest applied load to detectable AE among these six laminates. The ranking of the six laminate materials is different using different test methods. The most effective test method for predicting pad cratering susceptibility is inconclusive from this study.

Introduction
Pad cratering has become more prevalent with the switch to lead free solders and lead free compatible laminates. This mainly is due to the use of higher reflow temperature, stiffer Pb-free solder alloys, and the more brittle Pb-free compatible laminates. However, pad cratering is difficult to detect by monitoring electric resistance since pad cratering initiates before an electrical failure occurs.

Several methods have been developed to evaluate laminate materials' resistance to pad cratering. Pad-solder level tests include ball shear, ball pull and pin pull [1-3]. The detailed methods for ball shear, ball pull, and pin pull testing are documented in an industry standard IPC-9708 [4]. Bansal, et al. [5-6] proposed to use acoustic emission (AE) sensors to detect pad cratering during four-point bend test. Currently there is an industry-working group working on test guidelines for acoustic emission measurement during mechanical testing [7].

The four-point bend test is one of several test methods used for evaluating the susceptibility of new PCB boards to pad cratering, where cohesive damage can accumulate in the laminate well before electrical failure is affected. The attributes of four point bend testing that differentiate it from other methods (such as drop tests, cold pull tests, etc.) include that 1) the four-point bend can be run over different strain rates, 2) all solder ball joints within the inner span are under the same uniform bend load, and 3) in-test monitoring methods, such as resistance failure and acoustic emission can be added to the test as additional evaluation methods. The rate of strain will change the failure location. At low strain rates, fractures occur in the solder joint. At high rates of strain, pad craters will occur at the highest strain points, typically the corner pads of a BGA. One can consider 1000 microstrains per second a ballpark for the transition, although this simple rule of thumb does not factor in variables affecting the transition.

Both metal and composites will emit transient elastic waves when undergoing localized stress release (i.e., damage); this phenomena being known as Acoustic Emission. In addition to detecting local emissions from single sensors, arrays of sensors can be used to obtain arrival time information from the AE event and locate the origin. It has been speculated that a solder ball failure will emit once, while laminates will generate 4 or more distinct emissions before failure, although this lacks a sufficient level of confirmation.

The goals of this investigation are to compare the susceptibility of various laminates to pad cratering. The results of six different laminates' resistance to pad cratering using the ball pull, ball shear, and hot pin pull tests have been reported by authors in an earlier paper [8]. This paper presents the results of pad cratering susceptibility of laminates using the AE method under four-point bend and compares the AE results to the pad-solder level testing results.

Experiment

The laminate materials in this study are five Pb-free compatible high T_g laminates plus one dicy-cured non-Pb-free-compatible laminate. Laminate A is a high T_g un-filled dicy FR4, which is used as a control. Laminate B is a high T_g un-filled phenolic FR4; laminate C and laminate D are a high T_g filled phenolic FR4; laminate E is a high T_g filled mid-range-D_f phenolic FR4, and laminate F is a high T_g un-filled mid-range-D_f phenolic FR4.

The test coupon for this study is shown in Figure 1. The dimensions of the coupon are 7.2" (183mm) by 5" (127mm) with the PCB thickness of 0.059" (1.5mm). It is a 10-layer board with immersion silver surface finishing. Three daisy-chain BGA components assembled in the test vehicle are A-CABGA288-0.8mm-19mm-DC-LF305 (J3), A-PBGA324-1.0MM-23MM-DC-LF-305 (J4), and SDRAM DDR2 512M-bit 667MHz 1.8V 84-FBGA (U3). All test boards were pre-conditioned through a worst case scenario of Pb-free assembly environment, comprising 3, 5, or 7 reflow cycles @260°C peak for 10 seconds.

Bend testing was performed with an Instron uniaxial test machine with an 8800 series controller. The four point bend fixtures were made of hardened steel. Rubbing on the rounded bend rollers was mitigated by use of thin non-slip adhesive tape that prevented direct contact of the steel fixtures with the composite board. The bend test details are shown in Table 1. The bend test setup is shown in Figure 2.

The tests in this study were done at a rate of 5,000 microstrains per second in order to achieve pad craters. This fast rate resulted in tests less than 2 seconds long, so a set level of deflection was used rather than terminating the test once activity is detected. Initial measurements of the printed circuit board without components were done to determine the basic fracture level of the board. Board deflection was recorded by crosshead displacement and translated to load. Initial tests were correlated to strain level, but strain was not measured on every sample.

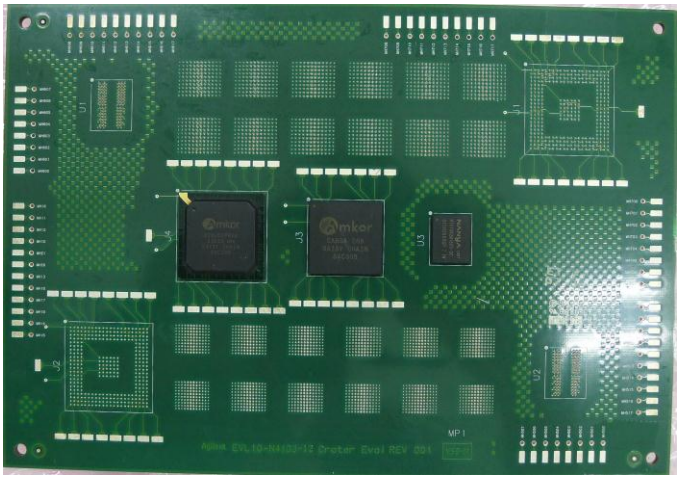

Figure 1: Test Coupon.

Table 1. Parameters of four-point bend test

Load Span	100 mm
Support Span	150 mm
Crosshead Speed	1.0 mm/sec
Number of AE sensors	4

Figure 2. Four-point bend setup

Figure 3 shows a test board in the fixture. Four AE sensors are under the clamp shown in Figure 3. To setup the 4-point bend testing, a bare board was tested to failure, plus a sample of each laminate was tested to electrical failure and AE failure respectively. With enough load, it can be expected that laminate boards will emit away from any stress rising due to solder balls. The first AE on boards without components was found to be at a deflection of 11 mm. This load level is well above the load levels under test of the populated boards. Testing bare boards before the populated boards is necessary for any new board laminate/layup or the substitution of lower frequency sensors.

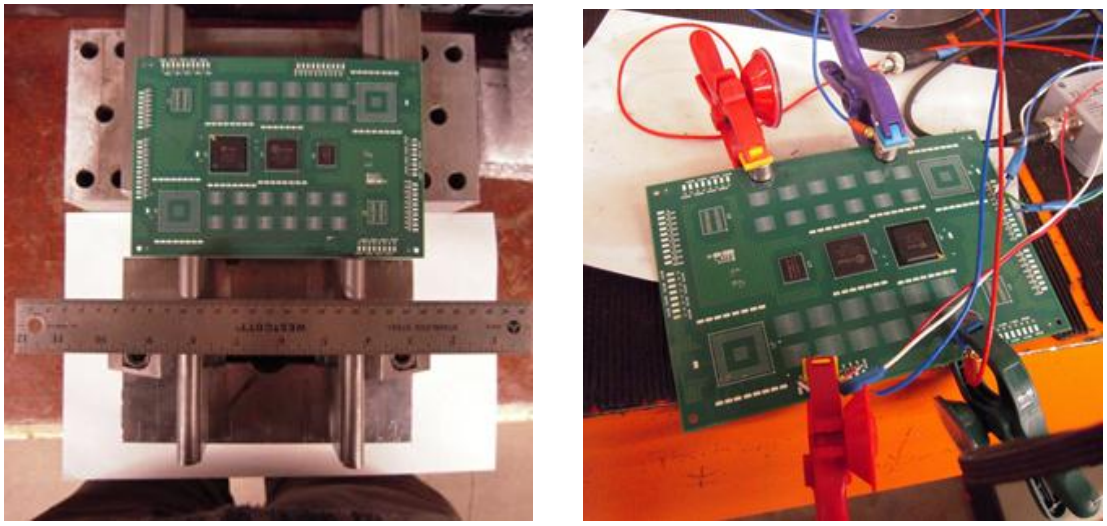

Figure 3. Test board in fixture and location of AE sensors.

All AE equipment used in this study is off-the shelf commercial offerings. A high end AMSY5 from Vallen-Systeme GmbH was used which provided enough versatility for multichannel low noise captures, 100-nanosecond global clock resolution of arrival times. AEP4 preamps were used.

AE sensors with resonant frequency of 650kHz and < 4.0mm aperture were selected. The high frequency of this AE sensor is optimally suited for capturing transient signals from composite boards of this dimension; the signals are all readily detectable without significant interference from signals reflected. The aperture size is a second consideration in sensor selection. A small aperture produces smaller time resolution, better defining the event location. Another consideration is that this sensor is highly effective against the lower frequency noises (such as vibration) which can contaminate the monitoring.

Event Criteria and Location Analysis

The three primary settings for AE detection in this type of AE system are threshold, rearm and duration discrimination testing. The former setting is to distinguish the beginning of the event, the latter two the end of the event. The transient capture allows a known beginning and end to an event, and detection threshold plays a role in both. Typical concerns of the

settings are sufficient sensitivity, noise rejection of low level noise, managing the trade-off between distinguishing events and allowing overlap from reflected events and getting as accurate an arrival time as possible. Fortunately, most of these are not issues in this board, sensor and strain rate combination. Thresholds between 30-40 dB AE are all viable with little noticeable difference. Lower levels may detect more background noise and more care is required at 30 dB to keep out external vibrational noise. As the threshold for detection is increased, the beginning of the wave is not captured as well, causing a small amount of error in location. A good starting point is a 40 dB threshold until there is more familiarity with the AE measurements. The end of the signal is also affected by threshold level. With this test, the strain rate is very high and the potential for event overlap will occur more readily at lower thresholds. Rearm times in the ballpark of 1 millisecond can be used without compromising distinct AE hit determination. If a 300 kHz sensor was substituted, the lower range of thresholds would be less of an option due to susceptibility to low frequency noise and overlapping signals. With this test, unlike other AE applications, these parameters are non-critical, at least with the 650 kHz sensor.

The largest experimental factors affecting the location results are choice of sensor array. Figure 3 shows the placement of the sensor array. It is desirable for all damage locations to be within the array as location errors increase significantly outside the sensor array. It is also important to have redundancy in the measurements. It takes 3 sensors to locate in a plane, 4 sensors give a redundancy factor that can help mitigate errant sensor results. More sensors would improve on this further, but at the cost of slowing testing. For positions, the sensors were placed just inside the 4 point bend far enough so that at peak deflection the sensors do not contact the 4 point bend fixtures and generate noise. Two of the most likely weak points on the board itself, the corners of the J4 package, sit close to the edge of the four point span and even closer to, if not outside the sensor array, make the coordinate location in this region much more error prone than other parts of the board.
The velocity for the laminates was determined in pretest for both orthogonal directions. Event builder timeouts were several times the expected time delay across the sensor array. A representative velocity is used for x and y coordinate determination with the understanding that it is a compromise velocity with regard to the asymmetric nature of composites. Simulated AE (Pencil Lead Breaks or PLB's) was performed in a test pattern, specifically the corners of all 3 chips (12 total positions), and showed consistent location within 1-3 mm of each corner. This was performed on all boards prior to testing. It is expected that simulated AE will locate better than real, damage based AE, although the converse can also be stated; that the real damage can almost always be expected to locate less well than the PLB. Figure 4 shows an example of the output of the AE test, with mapped location of AE events and signal amplitude vs time chart.

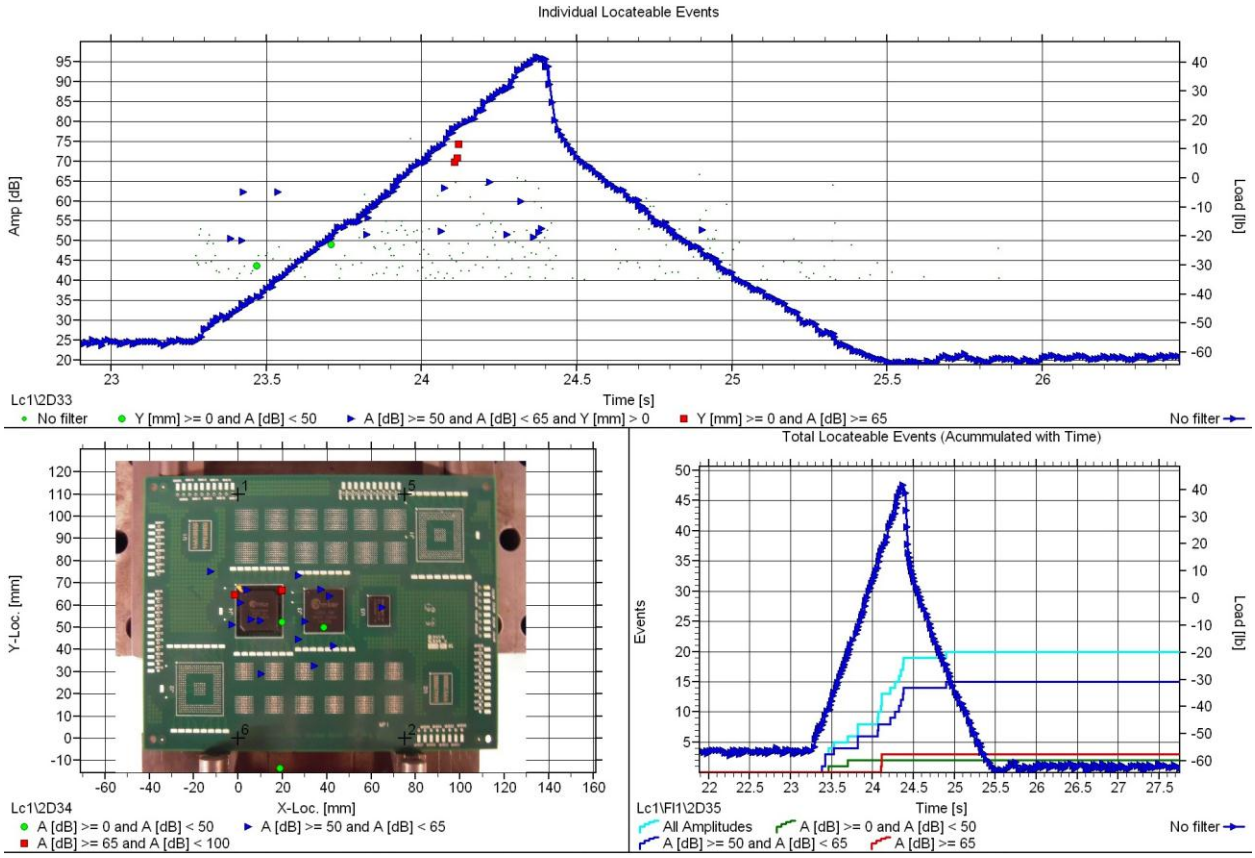

Figure 4. An example of AE Events

Figure 5 shows the location of AE events for different laminates. Though there are more AE events in some laminates than others, the majority of AE events concentrate in the largest BGA package (J4). It indicates that pad cratering is elevated with the larger size of BGA package. The stress concentration under the pads of the large BGA is higher than under the pads of the small BGA. It also shows that some AE events happened outside the package area. This means that not all AE events are associated with pad cratering.

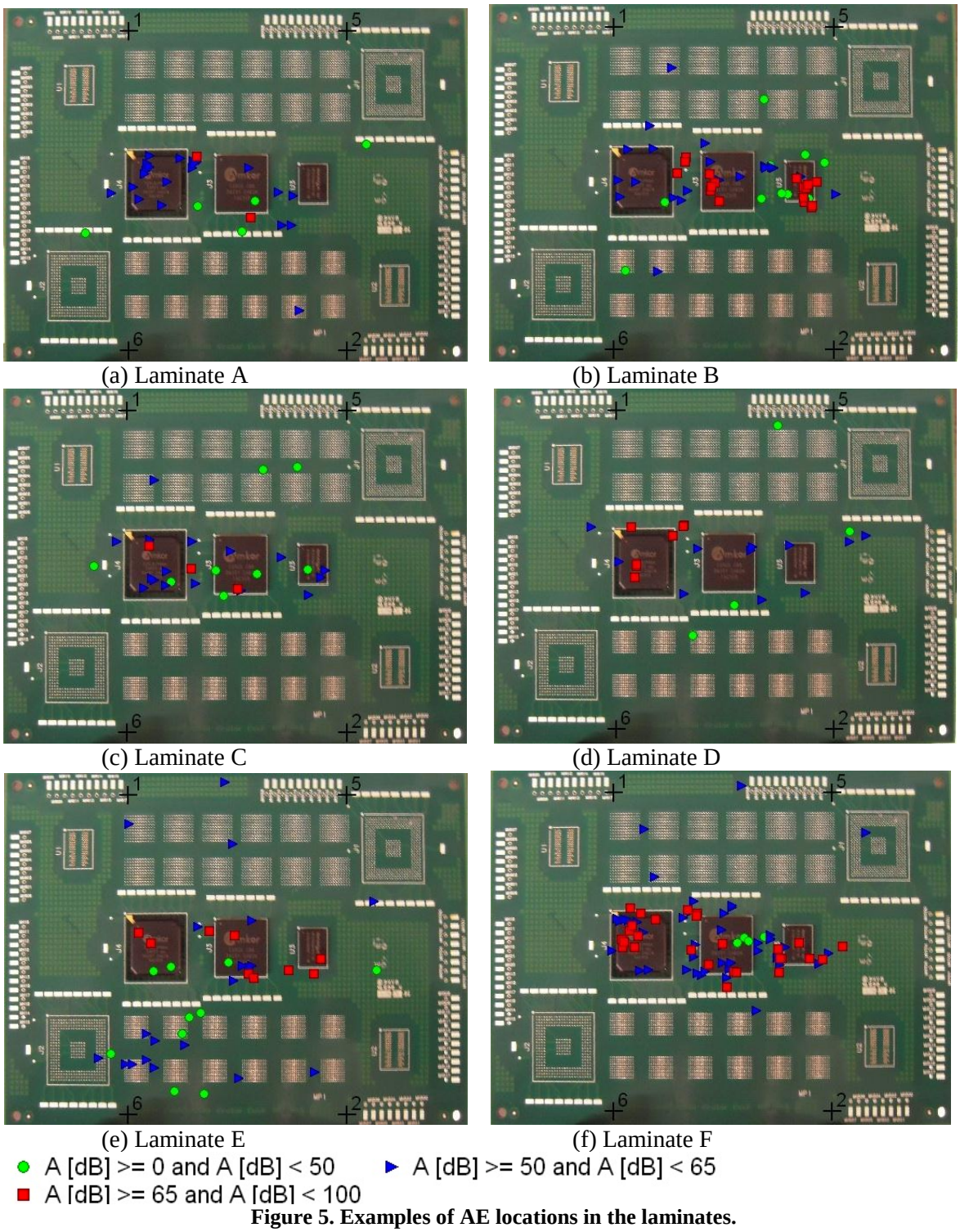

Figure 5. Examples of AE locations in the laminates.

Data Analysis

Though the acoustic emission method has been proven to detect pad cratering of PCB laminates [2, 3], no study has reported which AE parameters are good indicators for comparing the susceptibility of PCB laminates to pad cratering. In this analysis, we considered the following parameters as response variables:

1) The mean applied load when the first AE event with amplitude greater than 40 dB occurs
2) The mean applied load of the first four AE events with amplitude greater than 40 dB
3) The mean number of AE events with amplitude greater than 40 dB with applied load up to 30 lbs
4) The mean number of AE events with amplitude greater than 40 dB with applied load up to 50 lbs
5) The cumulative energy of all AE events with amplitude greater than 40 dB with applied load up to 30 lbs
6) The cumulative energy of all AE events with amplitude greater than 40 dB with applied load up to 50 lbs

Of the measured data, the peak decibel level of the first sensor of locatable AE events was used. The AE energy, a parameter which usually represents acoustic magnitude better than amplitude when errors arise was correlated to the amplitudes measured after tests and found to be close to 1:1 correlation.

There are 12 boards for each laminate, a total of 72 boards. Four boards of each laminate were pre-conditioned through 3, 5, and 7 reflow cycles at 260 °C peak temperature for 10 seconds. The boards subjected to 3 reflow cycles were used for AE test setup. No statistically significant difference between boards with 5 and 7 reflow cycles was found. Thus, eight boards for each laminate (consisting of 4 boards subjected to 5 reflow cycles and 4 boards subjected to 7 reflow cycles) were used for this analysis.

Fig. 6(a) shows there is no statistically significant difference in mean applied load at the first AE event with amplitude greater than 40 dB among these six laminates. Fig. 6 (b) shows there is no statistically significant difference in mean applied load at the first four AE events with amplitude greater than 40 dB among these six laminates. The purpose of using the average applied load of the first four AE events as a response variable is to reduce the variation because there is large variation in the applied load when the first AE event occurs. This result indicates that the lowest applied load to detectable AE may not be a good indicator for comparing laminates' resistance to pad cratering.

Fig. 7 shows that Laminate F is a frequent AE emitter as evidenced by the significant number of AE events with amplitude greater than 40 dB that occurred when both the applied load at 30 lbs and 50 lbs compared to other five laminates. Fig. 8 shows that Laminate F released significantly more energy than other laminates when both the applied load at 30 lbs and 50 lbs. Both the number of AE events at given applied load and the cumulative energy of AE events at given applied load indicates that Laminate F is prone to pad cratering.

Our empirical experience with laminates is that Laminate F is inferior and that Laminate A, our control laminate that is dicy-cured, is superior. Laminate F proved to be a frequent AE emitter, confirming our experience. The expected superiority of Laminate A is not evident; this may be because of degradation due to incompatibility of this laminate with the multiple high temperature reflows. The degradation with additional reflow cycles seen in the other test methods reported in our earlier paper [8] was not found, although with this test method we compared only 5 and 7 reflows.

Verification of pad cratering was done with cross-sections. To enhance the visibility of the pad craters, two methods were tried: powder filling and polarized light. Polarized light produced much more visible pad craters. The vast majority of the pad crater failures were, not surprisingly, at the corners of the largest BGA. Fig. 9 shows examples of pad cratering.

As indicated in Fig. 5, not all AE events are associated with pad cratering because some AE events are located outside of the package. Fig. 10 shows two examples of laminate cracks indicated by AE events, but not associated with pad cratering. The cross-sectioning results confirm this finding.

Table 2 compares results of various test methods for evaluating pad cratering. Note that the results of six different laminates' resistance to pad cratering using the ball pull, ball shear, and hot pin pull tests (please refer to our earlier paper [8]). This ranking of laminate materials shows quite a bit of inconsistency of results among the methods. No conclusion can be drawn at this time as to which test method is better able to distinguish the laminate materials' resistance to pad cratering.

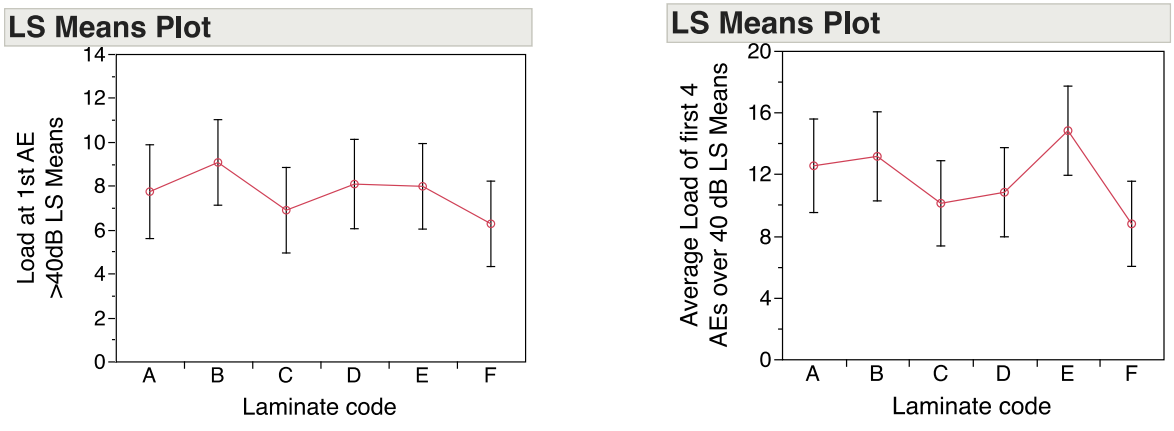

(a) (b)

Figure 6. (a) The applied load at first locatable AE event with amplitude greater than 40 dB, (b) Average applied load when first four AE events with amplitude greater than 40 dB.

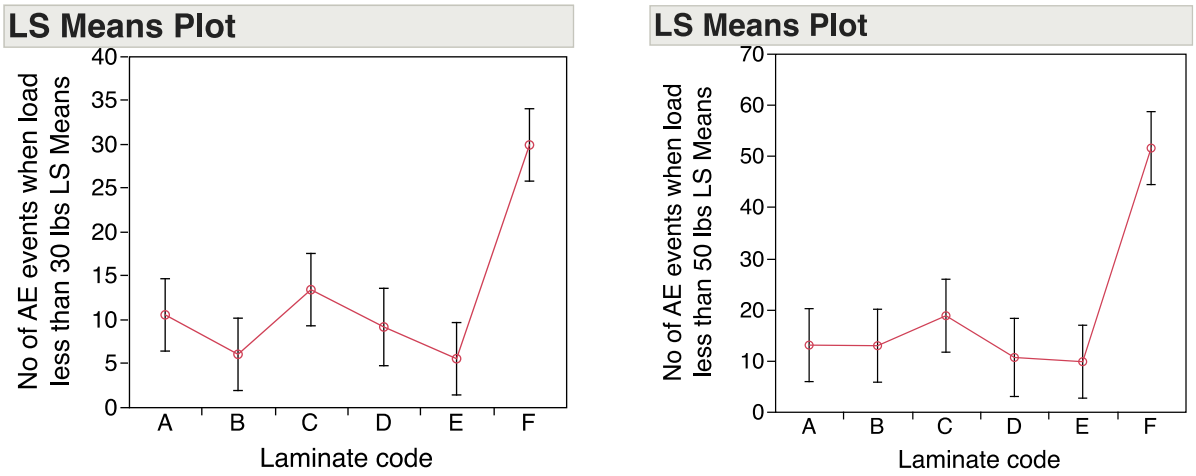

(a) (b)

Figure 7. (a) Number of AE events with amplitude greater than 40 dB when the applied load is 30 lbs, (b) Number of AE events with amplitude greater than 40 dB when the applied load is 50 lbs.

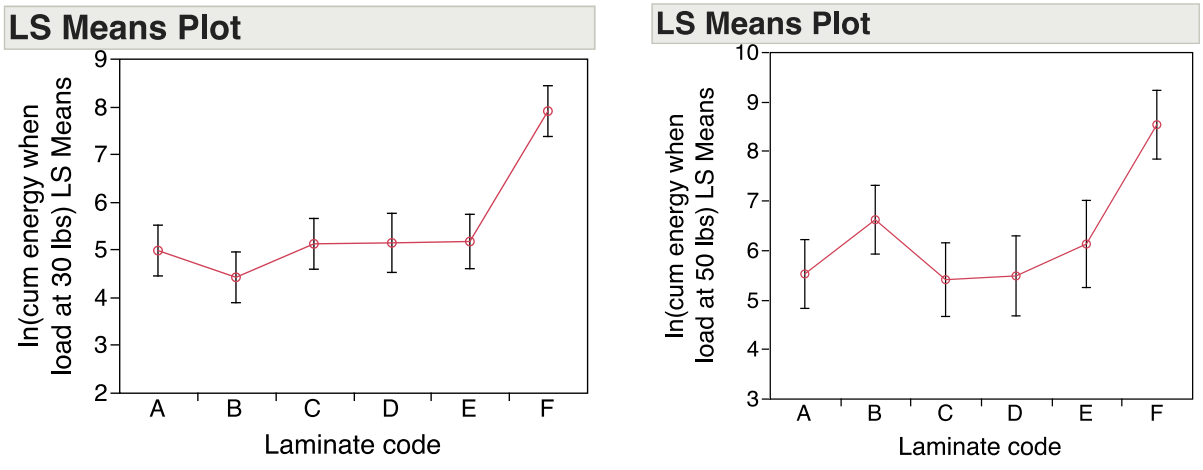

(a) (b)

Figure 8. (a) natural log of cumulative energy of all AE events with amplitude greater than 40 dB when the applied load is less than 30 lbs, (b) natural log of cumulative energy of all AE events with amplitude greater than 40 dB when the applied load is less than 50 lbs.

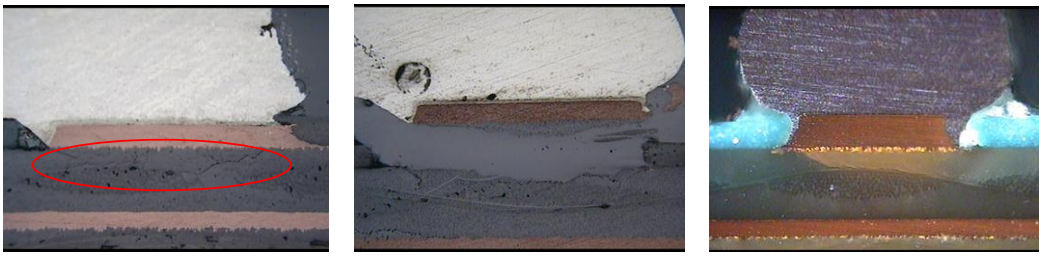

(a) (b) (c)

Figure 9. Cross-section examples: (a) standard cross-section, (b) powder filling, (c) polarized light on right

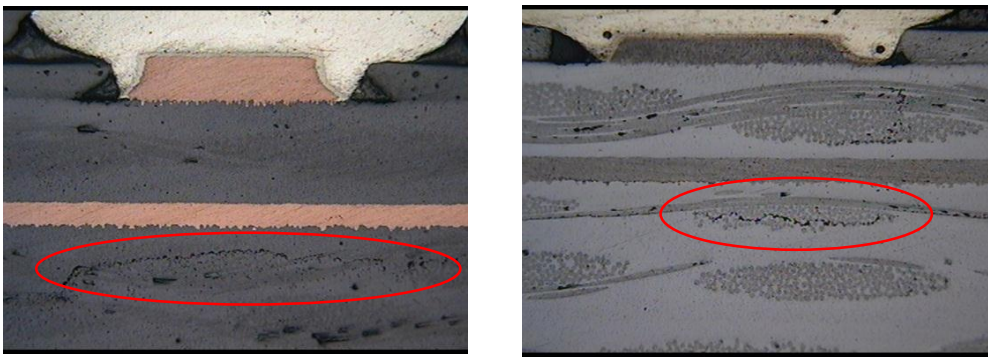

Figure 10. Examples of AE events not associated with pad cratering

Table 2: Ranking of Laminate Materials

Laminate Materials	Hot pin pull test	Cold ball pull test	Ball shear test	Board level drop test	4-point bend test with AE
A	1	1	1	1	1
B	2	3	2	3	1
C	3	4	2	2	1
D	4	2	2	4	1
E	5	2	2	2	1
F	5	5	3	3	2

Conclusions

Pad cratering susceptibility of five Pb-free compatible laminates and one dicy-cure non-Pb-free-compatible laminate was evaluated using 4-point bend testing with acoustic emission. Cross-sectioning results confirm that the acoustic emission method is a viable tool to detect pad craters during the 4-point bend test. However, not all AE events are associated with pad cratering. Laminate cracks in locations away from the component or between layers are detected by the AE method.

Location analysis shows the majority of AE events concentrate in the largest BGA package in the test vehicle. It indicates that pad cratering is elevated with the larger size of BGA package, which can be explained by the higher stress concentration under the pads of large BGAs than under the pads of small BGAs.

Both the number of AE events and the cumulative energy of AE events at a given applied load indicates that Laminate F is prone to pad cratering, confirming our experience. However, there is no statistically significant difference in the lowest applied load to detectable AE among these six laminates. Thus, the lowest applied load to detectable AE may not be a good indicator for comparing laminates' resistance to pad cratering. It is recommended to use the number of AE events and the cumulative energy of AE events at a given applied load to evaluate laminates' resistance to pad cratering.

The ranking of the six laminate materials is different among the pad-solder level tests, the drop test, and the 4-point bend test with acoustic emission. The most effective test method for predicting pad cratering susceptibility is inconclusive from this study.

Acknowledgements

The authors would like to thank Dr. Jianbiao Pan of California Polytechnic State University, San Luis Obispo, for technical support; and Allen Green, formerly of Acoustic Technology Group, for AE expertise.

References

[1] Dongji Xie, Dongkai Shangguan, and Helmut Kroener, "Pad Cratering Evaluation of PCB," Proceedings of IPC APEX Expo, 2010.
[2] Mudasir Ahmad, Jennifer Burlingame, and Cherif Guirguis, "Validated Test Method to Characterize and Quantify Pad Cratering Under BGA Pads on Printed Circuit Boards", Proceedings of IPC APEX Expo, 2008.
[3] Mudasir Ahmad, Jennifer Burlingame, and Cherif Guirguis, "Comprehensive Methodology To Characterize And Mitigate BGA Pad Cratering In Printed Circuit Boards", Journal of SMTA, January 2009.
[4] IPC 9708: Test Methods for Characterization of Printed Board Assembly Pad Cratering, 2010.
[5] Anurag Bansal, Gnyaneshwar Ramakrishna, and Kuo-Chuan Liu, "A New Approach for Early Detection of PCB Pad Cratering Failures", Proceedings of IPC APEX Expo, 2011.
[6] Anurag Bansal, Cherif Guirguis, and Kuo-Chuan Liu, "Investigation of Pad Cratering in Large Flip-Chip BGA using Acoustic Emission", Proceedings of IPC APEX Expo, 2012.
[7] IPC-9709 working draft, "Test Guidelines for Acoustic Emission Measurement during Mechanical Testing," 2012.
[8] Wong Boon San and Julie Silk, "Pad Cratering Susceptibility," Proceedings of SMTA International Symposium, 2012.